Hindawi
Advances in Materials Science and Engineering
Volume 2019, Article ID 8970689, 8 pages
https://doi.org/10.1155/2019/8970689

Research Article

Study on Grinding Mechanism of Brake Pad with Copper Matrix Composites for High-Speed Train

Chong Su, Chao Wang, Xiaoshuai Sun, and Xinghua Sang

School of Mechanical Engineering, Dalian Jiaotong University, 794 Huanghe Road, Dalian 116028, Liaoning, China

Correspondence should be addressed to Chong Su; chn_s@126.com

Received 25 June 2018; Revised 30 September 2018; Accepted 28 January 2019; Published 25 February 2019

Academic Editor: Hongtao Zhu

The processing mechanism of copper matrix composites is very complex, for the particle phase and lubricating phase are randomly distributed in the copper matrix phase, and the characteristics of the three phases are completely different. Aiming at understanding the chip formation and the influence of each phase of the material on the workpiece surface morphology, a single abrasive grain cutting experiment is carried out. Experiment results show that the cutting force increases with the increase in the cutting depth, but the increase amplitude is smaller. Extrusion of the abrasive particles causes plastic deformation of the copper matrix phase and brittle fracture of the particle phase and graphite phase. It results in the defects on the groove surface, such as pits, collapses and cracks, and holes. The brittle fracture of the graphite phase and the breaking and falling off of the particle phase block the plastic deformation of the copper alloy, which makes the copper alloy not forming ductile chips. The chip is mainly powdery. It shows that the brittle fracture is the main removal form of the brake pad material. The copper matrix phase on the surface of the groove produces obvious plastic deformation. The plastic deformation at the bottom is larger and has a certain degree of fibrosis appearing.

1. Introduction

A brake pad with copper matrix composites is the main type of high-speed train brake pads. This kind of brake pad has copper as a binder, adding a certain proportion of alloy elements, friction components (silicon carbide, alumina, etc.), and lubricating components (graphite, molybdenum disulfide, etc.). It is manufactured by the powder metallurgy process. After pressing, sintering, and shaping processes, the size and surface integrity requirements of the product can be achieved through the grinding process. The particle phase and the lubricating phase are randomly distributed in the copper matrix, and the characteristics of the three are completely different, so its processing mechanism is very complex.

Machinability of particle-reinforced metal matrix composites has been extensively studied [1–3]. Dong et al. [4] studied the grinding mechanisms of high-volume fraction SiCp/Al composites by ultrasonically assisted grinding with an electroplated diamond wheel. Their study shows that material removal in grinding of SiCp/Al composites is dominated by SiC particle fracture. Compared with conventional grinding, ultrasonically assisted grinding of SiCp/Al composites results in similar surface integrity in terms of surface roughness and subsurface damage but a much lower grinding force (35–50% lower). Dabade and Jadhav [5] tried to improve the machinability of Al/SiCp-MMCs and surface quality by hot machining. The experiments were carried out under dry cutting conditions. PVD-coated carbide inserts were used. The experimental results shows that feed, depth of cut, and preheating temperature have significant influence on cutting force, feed force, thrust force, surface roughness, and microhardness variation beneath the machined surface. Shoba et al. [6] studied the influence of machining parameters, e.g., cutting speed, feed, and depth of cut on the cutting force. The results prove that the cutting force decreases with the increase in the weight percentage of the reinforcement. It is analyzed that this is probably due to the dislocation densities generated from the thermal mismatch between the reinforcement and the matrix. Kumar et al. [7]

studied the machining aspects of Al/SiCp-MMC using the wire-cut electric discharge machining process. Their study recommends optimal process parameters such as pulse on time, pulse off time, spark gap voltage, peak current, wire tension, and wire feed rate for effective machining of Al/SiCp-MMC. Ghandehariun et al. [8, 9] presented a micromechanical finite element analysis developed for simulation of MMC machining. The model can simulate the behavior of all main components that distinguish the MMC, namely, the matrix, particles, and particle-matrix interface during the process, so the debonding and fracture in the particles and different scenarios of tool-particle interactions can be studied using the proposed model. Pramanik et al. [10] investigated experimentally the effects of reinforcement particles on the machining of MMCs. The results show that the surface residual stresses on the machined MMC are compressive, the surface roughness is controlled by feed, and particle pullout influences the roughness when the feed is low. Chen et al. [11] developed a three-dimensional finite element end milling model with an equivalent homogenous material model, which was drawn from the quasi-static and split-Hopkinson pressure bar tests. Their model is verified by milling experiments, and it is found that the predicted milling forces are consistent with those in milling experiments. Kumar et al. [12] studied the dry turning characteristics of in situ Al-4.5%Cu/TiC metal matrix composites using uncoated ceramic inserts. The experimental results indicate that the length of the chip and the number of chip curls increase with an increase in the cutting speed at the given feed rate and depth of the cut, and a C-type chip changes to a segmental-type chip was influenced by the weight percentage of reinforcement. Zhou et al. [13] studied the machinability, including machined surface, edge quality, and the distribution of the subsurface residual stress, during the orthogonal cutting of high-volume fraction SiCp/Al composites by both finite element analysis and experiments. Their study highlights the important role of the fracture model of SiC particles on surface finish and the edge quality.

Because of the complexity and uncertainty of the grinding wheel structure, the material removal mechanism in grinding is more complex than that in cutting [14]. The single abrasive grain cutting is one of the main methods for the research of the grinding mechanism at present, such as chip formation, grinding force, and abrasive wear in the grinding process [15–17]. Su et al. [18] simulated the process of single abrasive grain cutting particle-reinforced Cu-matrix composites with a small volume fraction of the particle phase. It is found that the plastic removal of the Cu-matrix is still the main removal form of the composite, but the existence of the reinforced particle phase affects the cutting deformation behavior and the chip morphology. Tawakoli et al. [19] studied the material removal mechanism in grinding of alumina by the single abrasive grain scratch experiment. It is found that the material pile up decreases with higher cutting speed. The transition from ductile to brittle mode of material removal occurs earlier in higher cutting speeds. Singh et al. [20, 21] developed a model of specific ploughing energy in mild steel using single grit scratch tests and investigated the effects of grinding process parameters on specific ploughing energy. It is found that the grain size and depth of cut have significant effect on the ploughing phenomenon. Specific ploughing energy is regarded as an important component of total specific energy. At a very low cutting depth, this part becomes more important. Chen and Öpöz [22] studied the material removal mechanism in grinding with single- and multiple-edge CBN grit scratch tests and characterized the material removal by considering the material pile up ratio, material removal specific energy, and acoustic emission feature during the scratching process. The experimental results show that the cutting action is more effective in single-edge scratches while ploughing action is more dominant in the multiple-edge scratches. Denkena et al. [23] investigated the material removal mechanisms of reinforced concrete by means of single grain scratch experiments. The experiment results shows that, with regard to process efficiency and stability, the cutoff grinding wheel with higher diamond grain concentration and deterministic distribution performs best in the given field of application.

The working surface of the brake pad requires a certain coefficient of friction, so it is different from the usual grinding process that it is necessary to get a high surface finish. The surface of the brake pad after grinding is generally required to have a certain surface roughness and less surface defects. In this paper, the single abrasive grain cutting method is used to study the grinding mechanism of a copper matrix composite brake pad. The chip formation and the influence of each phase of the material on the chip morphology and surface quality are analyzed.

2. Experimental Method

A triangle single point diamond cutting tool and its clamping device are shown in Figure 1. The clamping device is disk shaped; its outer diameter is 300 mm, and the inner diameter is 75 mm. Two U-shaped grooves are designed symmetrically at the circumference of the base disk for the installation of single point diamond cutting tools and balance blocks. The material of the base disk is L12 aluminum alloy. In the design of cutting tools, the design ideas of the cemented carbide indexable insert are used for reference. The diamond particles are fixed on the three vertices of the triangular cutting tool through the brazing process. The cutting tool has a "Y" slot on one side of it, which is used to locate the tool, and is fixed on the disc by a wedge. The triangular cutting tool can be indexable, and it is easy to replace when the abrasive particles are damaged during the experiment.

The brake pad in the experiment is triangular and is clamped with a parallel-jaw vice, as shown in Figure 2. It is prepared by using the powder metallurgy method. The friction phase of the brake pad material is Al_2O_3 and SiO_2, the lubricating phase is graphite, and the matrix phase is copper alloy (including certain Fe and Cr). The cutting force of single diamond particles is measured by using a SPC-C4M dynamometer. The groove morphology was observed by using a Leica microscope, and the surface profile of the

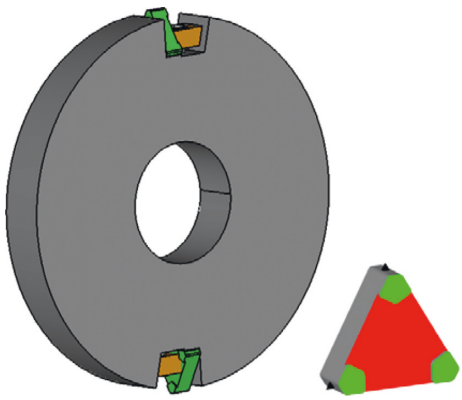

Figure 1: Single point diamond cutting tool and clamping device.

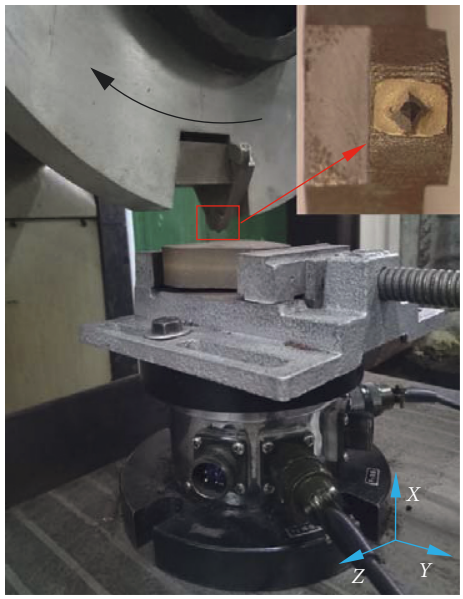

Figure 2: Single point diamond abrasive grain cutting experiment device.

groove was constructed. The morphology of the groove surface and cross section were also observed by using a scanning electron microscope.

The experiment includes two parts. First, the brake pad surface is grinded to obtain a flat surface with a wheel speed of 1440 r/min and a grinding depth of 10 μm and then the cutting experiment of a single diamond abrasive grain is carried out so that the groove morphology of single abrasive cutting can be observed better. The grinding depth is the most important process parameter in the brake pad shape modification. Therefore, the experiment focuses on the influence of the cutting depth of the abrasive grains on the surface morphology of the workpiece. When the spindle speed is 1440 r/min, the cutting depths of single diamond abrasive particles are 50 μm, 70 μm, 90 μm, and 110 μm respectively.

Figure 3: Surface of the brake pad after grinding.

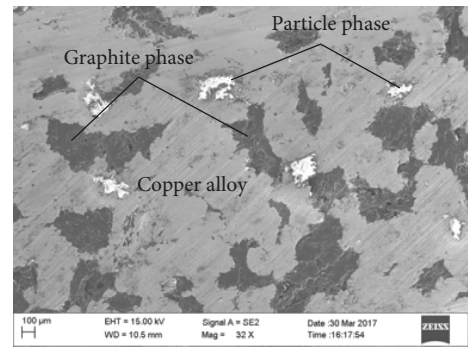

Figure 4: Surface microstructure of the brake pad.

3. Experimental Results and Analysis

3.1. Grinding Surface. Before processing, the surface of the brake pad is dark grey. After grinding, the surface is mainly bright yellow with some black spots, as shown in Figure 3. The bright yellow is copper alloy, and the black spots are graphite phase. The composition of the surface is observed under the electron microscope, as shown in Figure 4; it can be seen that there are some bright silver particles in the copper matrix. It shows that, under the action of grinding force, the soft copper alloy produces plastic deformation and some copper alloys cover on the graphite phase and particle phase, hole defects are produced at the interface between the particle phase and the copper alloy matrix, and lamellar fragmentation defects are produced on the surface of the graphite phase.

When grinding the surface of the brake pad, it does not produce spark that appears while grinding the ordinary metal material but produces powdery chips that spatter along the grinding wheel. It indicates that the chip temperature does not reach the melting point of the copper matrix composite. There are two reasons about it. On the one hand, copper matrix composite materials contain a certain volume fraction of graphite and hard particles, and their melting points are much higher than the melting point of metal materials. On the other hand, although the existence of graphite phase and particle phase improves the frictional properties of materials, the fracture strength of

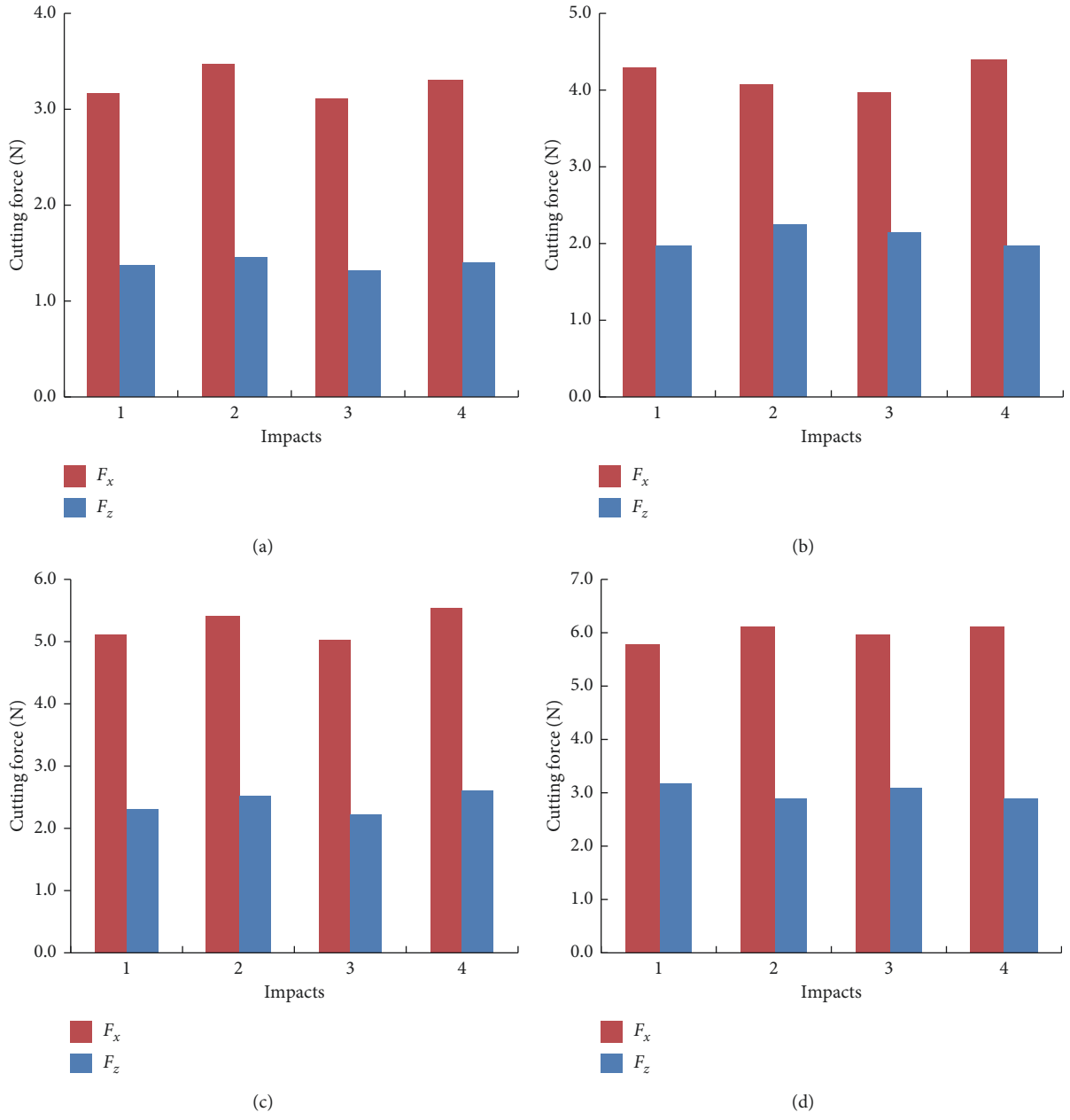

Figure 5: Cutting forces under different cutting depths. (a) $a_p = 50\,\mu$m. (b) $a_p = 70\,\mu$m. (c) $a_p = 90\,\mu$m. (d) $a_p = 110\,\mu$m.

materials becomes low, which is easier to remove than general metal materials and has less grinding force and less grinding heat. So there is no spark appearing at the grinding contact area.

3.2. Analysis of Single Abrasive Grain Cutting

3.2.1. Cutting Force. In the experiment, the shaft frequency of the grinder spindle is 24 Hz and the acquisition frequency of the cutting force is 200 Hz. The normal cutting force and tangential cutting force the single point diamond tool are measured. The signals are periodic impact signals. The Y direction is the axial direction of the rotary cutting device, and there is no feed motion in the direction. The shape of the abrasive grain is nearly symmetrical in the ZX plane, which makes the forces on both sides of the abrasive grains almost equal, so F_y is very small, and its average value is close to zero. Figure 5 shows the cutting forces in the signal stabilization stage under different cutting depths. F_x is the normal cutting force, and F_z is the tangential cutting force. It can be seen that the normal cutting force of the single abrasive grain is greater than the tangential cutting force, which is mainly due to the larger rake angle of the abrasive grain when the scratching occurs, which results in the normal component of cutting force greater than the tangential component. The curves of the mean value of cutting force under different cutting depths are shown in Figure 6. It can be seen that the

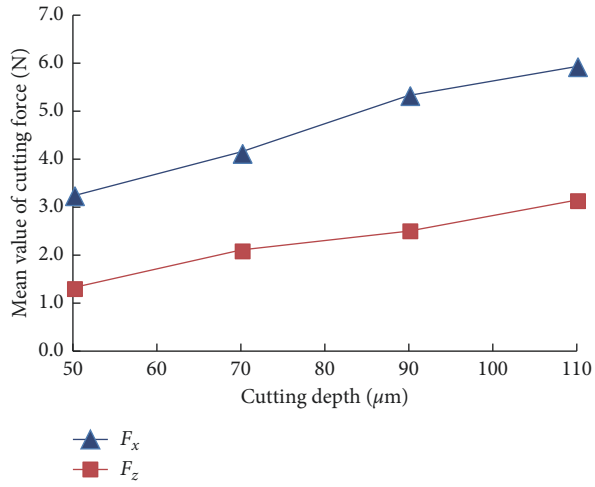

Figure 6: Mean value of the cutting force under different cutting depths.

cutting force increases with the increase of the cutting depth, but the amplitude of the change is small. The reason is that the graphite content of the brake pad material is high, while the strength of graphite itself is low, and it is easy to break under the action of grinding force, so the cutting force increases little with the increase in the cutting depth.

3.2.2. Groove Surface Morphology. The workpiece is cleaned with anhydrous alcohol for 10 minutes in the ultrasonic cleaning machine and then is dried quickly with a blower. The micromorphology of groove surface is observed by using the Leica microscope, and the contour of scratch surface is constructed, as shown in Figure 7. It can be seen that both sides of the grooves and the bottom are relatively rough, and there are various forms of defects, but there is no obvious uplift on both sides of the groove. It indicates that the brake pad material is mainly removed by the brittle fracture, while the plastic deformation of the copper matrix is not dominant. This is mainly due to the large volume fraction of graphite phase and particle phase. The brittle fracture of the graphite phase and the falling of the particle phase block the plastic deformation behavior of the copper matrix.

Figure 8 shows the scratch surface defects observed by using the scanning electron microscope. It can be seen that there are pits, collapses, cracks, and broken particles on the groove surface. The extrusion of the abrasive grain makes the exposed graphite phase broken, forming an irregular pit, as shown in Figure 8(a). Under the action of the cutting force, the graphite phase in the subsurface layer breaks down, causing the copper matrix to collapse and forming a larger crack, as shown in Figure 8(b). The particle phase on the cutting path is crushed by the diamond abrasive grain, and the broken particles are pressed into the interior of the copper matrix, as shown in Figure 8(c).

3.2.3. Groove Cross-Sectional Morphology. From the fracture morphology of the grooves shown in Figure 9, it can be seen that the morphology is basically caused by the brittle fracture, and there is no lateral uplift happening on both sides of the grooves like cutting plastic metal material. The reason is that the formation of the above surface defects makes the copper alloy matrix of the cutting layer does not complete plastic deformation before being removed. As a result, powdery chips are formed in the abrasive grain cutting, without the formation of a ductile chip and no spark appearing.

In order to more clearly observe the morphology of each phase in the deformation layer of the brake pad, the sample section was polished, and the surface of the polishing surface was corroded for 10 minutes with ferric chloride hydrochloric acid solution to remove the plastic layer produced by the polishing process, revealing a clear deformation layer structure. Figure 10 shows the microstructure of the groove surface layer under the cutting depth of 110 μm; it can be seen that the copper matrix on the groove surface has obvious plastic deformation, the thickness of deformation layer is about 5 μm to 10 μm, the deformation at the bottom is larger, and there is a certain degree of fibrosis.

4. Conclusions

(1) The brake pad material contains a certain volume fraction of graphite and particle phase, which leads to the decrease of the fracture strength. When grinding, the material is relatively easy to remove and produces less heat, which makes the grinding temperature lower than the melting point of the material. Therefore, the solid powdery chip is produced at the grinding contact area, and the powdery chip is not melted into sparks.

(2) There are pits, collapses, cracks, and broken particles on the groove surface. The extrusion of the abrasive particles causes the exposed graphite phase to break down and form an irregular pit, and the graphite phase in the subsurface layer is broken under the action of cutting force, resulting in the collapse of the copper matrix on the surface and the formation of large cracks. The particle phase on the cutting path is crushed by the abrasive grain, and the broken particles are pressed into the interior of the copper matrix.

(3) The brittle fracture of the graphite phase and the breaking and falling off of the particle phase block the plastic deformation of the copper alloy, which makes the copper alloy do not form ductile chips. Therefore, the chip is mainly powdery. It shows that the brittle fracture is the main removal form of the composite brake pad.

The volume fraction of each phase is an important factor affecting chip formation. The larger the volume fraction of graphite phase and particle phase, the easier the material is removed by the brittle fracture but not plastic deformation. In future work, the critical volume fraction of these two phases to block the plastic deformation behavior of copper matrix will be studied.

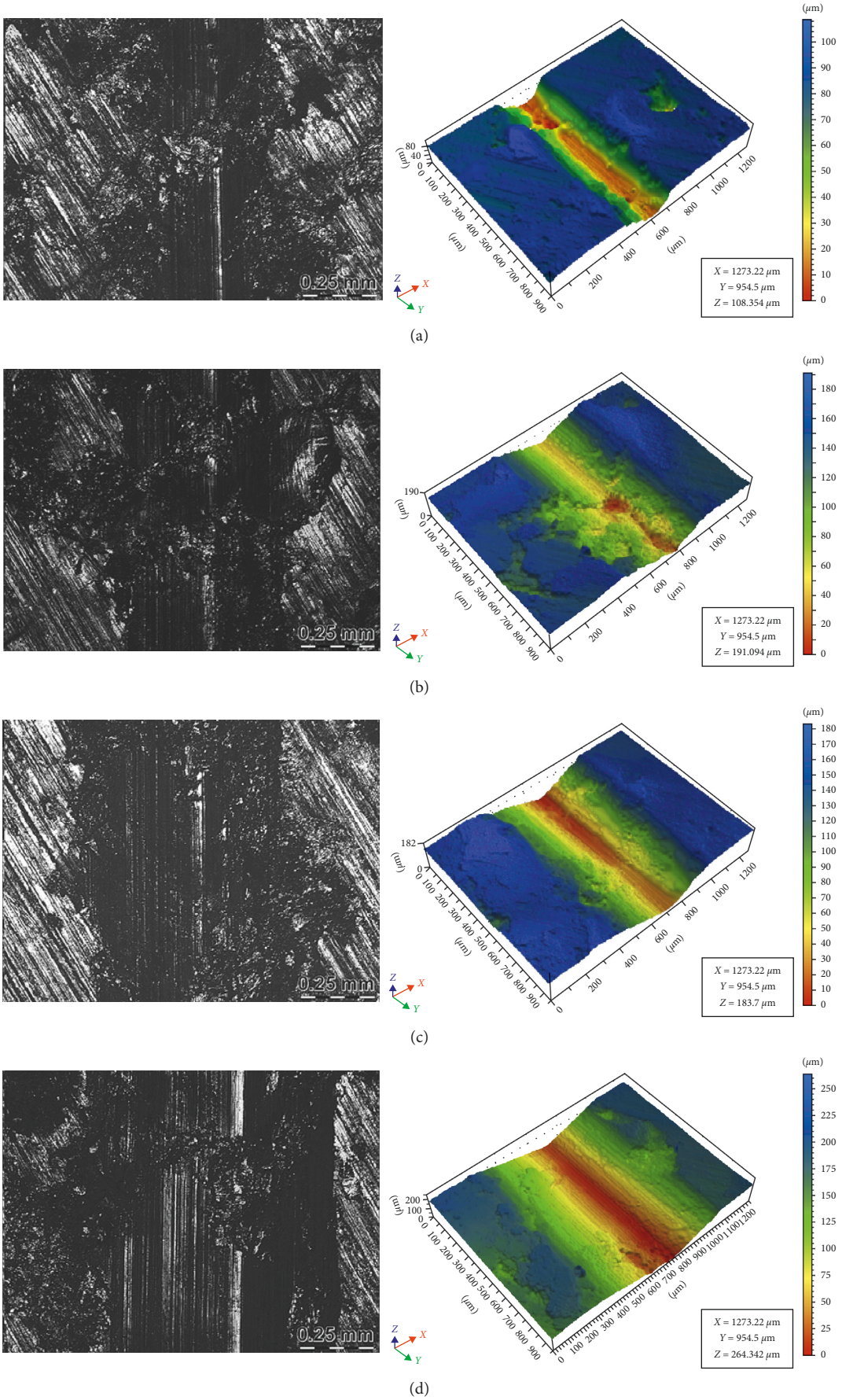

Figure 7: Surface morphology and contour of the grooves under different cutting depths. (a) $a_p = 50\,\mu m$. (b) $a_p = 70\,\mu m$. (c) $a_p = 90\,\mu m$. (d) $a_p = 110\,\mu m$.

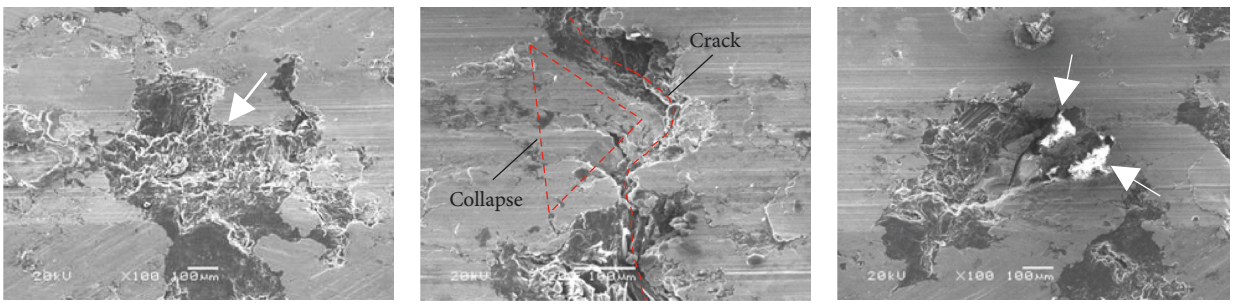

(a) (b) (c)

Figure 8: Surface defects of the grooves. (a) Irregular pit. (b) Collapse and crack. (c) Broken particle.

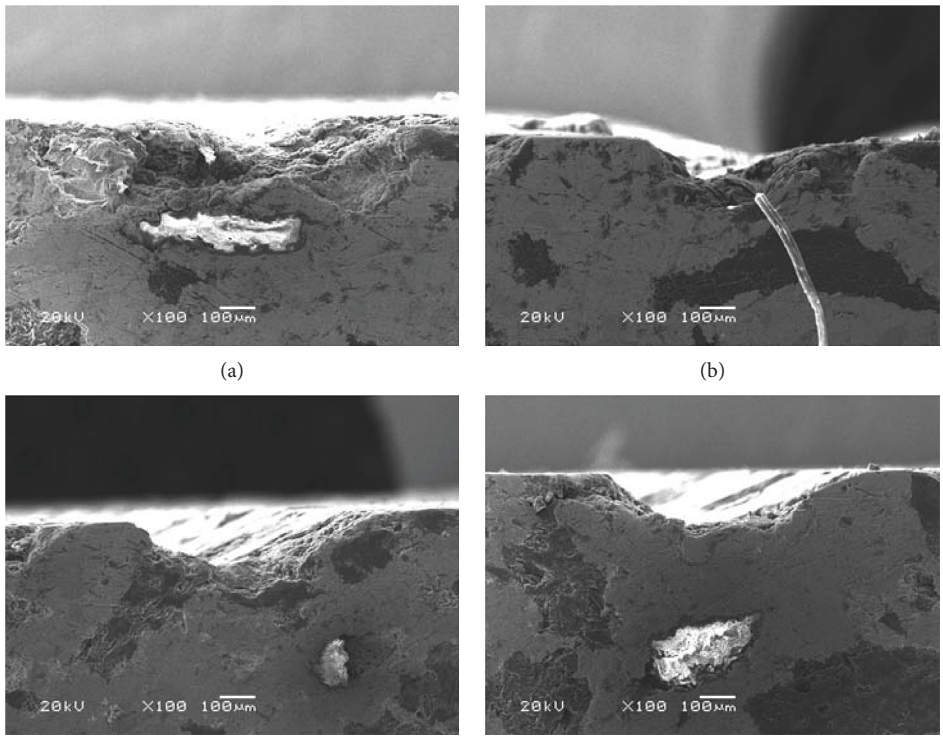

(a) (b)

(c) (d)

Figure 9: Fracture morphology of grooves. (a) $a_p = 50\,\mu$m. (b) $a_p = 70\,\mu$m. (c) $a_p = 90\,\mu$m. (d) $a_p = 110\,\mu$m.

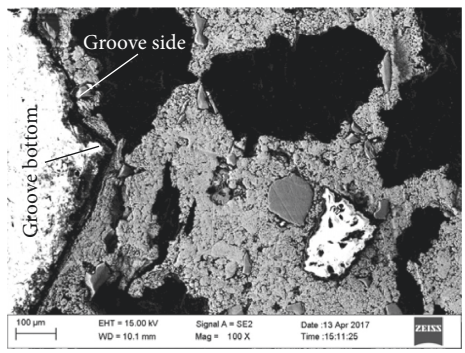

Figure 10: Microstructure of the groove surface layer.

Data Availability

The data used to support the findings of this study are available from the corresponding author upon request.

Conflicts of Interest

The authors declare that they have no conflicts of interest.

Acknowledgments

The authors thank their project research partners and fund support units. The work was supported by the Natural Science Foundation of Liaoning Province (201602136), National Basic Research Program of China (2015CB654802), and National Science and Technology Major Project (2018ZX04041001).

References

[1] R. Sekhar and T. P. Singh, "Mechanisms in turning of metal matrix composites: a review," *Journal of Materials Research and Technology*, vol. 4, no. 2, pp. 197–207, 2015.

[2] C. J. Nicholls, B. Boswell, I. J. Davies, and M. N. Islam, "Review of machining metal matrix composites," *International Journal of Advanced Manufacturing Technology*, vol. 90, no. 9–12, pp. 2429–2441, 2016.

[3] D. D. Kanta, P. C. Mishra, S. Singh, and R. K. Thakur, "Tool wear in turning ceramic reinforced aluminum matrix composites—a review," *Journal of Composite Materials*, vol. 49, no. 24, pp. 2949–2961, 2015.

[4] Z. Dong, F. Zheng, X. Zhu, R. Kang, B. Zhang, and Z. Liu, "Characterization of material removal in ultrasonically assisted grinding of SiCp/Al with high volume fraction," *International Journal of Advanced Manufacturing Technology*, vol. 93, no. 5–8, pp. 2827–2839, 2017.

[5] U. A. Dabade and M. R. Jadhav, "Experimental study of surface integrity of Al/SiC particulate metal-matrix composites in hot machining," *Procedia CIRP*, vol. 41, pp. 914–919, 2016.

[6] C. Shoba, N. Ramanaiah, and D. Nageswara Rao, "Effect of reinforcement on the cutting forces while machining metal matrix composites—an experimental approach," *Engineering Science and Technology, an International Journal*, vol. 18, no. 4, pp. 658–663, 2015.

[7] H. Kumar, A. Manna, and R. Kumar, "Modeling and desirability approach-based multi-response optimization of WEDM parameters in machining of aluminum metal matrix composite," *Journal of the Brazilian Society of Mechanical Sciences and Engineering*, vol. 40, no. 9, p. 458, 2018.

[8] A. Ghandehariun, H. A. Kishawy, U. Umer, and H. M. Hussein, "Analysis of tool-particle interactions during cutting process of metal matrix composites," *International Journal of Advanced Manufacturing Technology*, vol. 82, no. 1–4, pp. 143–152, 2015.

[9] A. Ghandehariun, H. A. Kishawy, U. Umer, and H. M. Hussein, "On tool–workpiece interactions during machining metal matrix composites: investigation of the effect of cutting speed," *International Journal of Advanced Manufacturing Technology*, vol. 84, no. 9–12, pp. 2423–2435, 2016.

[10] A. Pramanik, L. C. Zhang, and J. A. Arsecularatne, "Machining of metal matrix composites: effect of ceramic particles on residual stress, surface roughness and chip formation," *International Journal of Machine Tools and Manufacture*, vol. 48, no. 15, pp. 1613–1625, 2008.

[11] X. Chen, L. Xie, X. Xue, and X. Wang, "Research on 3D milling simulation of SiCp/Al composite based on a phenomenological model," *International Journal of Advanced Manufacturing Technology*, vol. 92, no. 5–8, pp. 2715–2723, 2017.

[12] A. Kumar, M. M. Mahapatra, and P. K. Jha, "Effect of machining parameters on cutting force and surface roughness of in situ Al–4.5%Cu/TiC metal matrix composites," *Measurement*, vol. 48, no. 2, pp. 325–332, 2014.

[13] L. Zhou, C. Cui, P. F. Zhang, and Z. Y. Ma, "Finite element and experimental analysis of machinability during machining of high-volume fraction SiCp/Al composites," *International Journal of Advanced Manufacturing Technology*, vol. 91, no. 5–8, pp. 1935–1944, 2016.

[14] L. D. Zhu, Z. C. Yang, and Z. Li, "Investigation of mechanics and machinability of titanium alloy thin-walled parts by CBN grinding head," *International Journal of Advanced Manufacturing Technology*, vol. 100, no. 9–12, pp. 2537–2555, 2018.

[15] M. Akbari, M. Kliuev, J. Boos, and K. Wegener, "Temperature and force measurements in single diamond scratch tests," *International Journal of Advanced Manufacturing Technology*, vol. 96, no. 9–12, pp. 4393–4405, 2018.

[16] T. T. Öpöz and X. Chen, "Experimental investigation of material removal mechanism in single grit grinding," *International Journal of Machine Tools and Manufacture*, vol. 63, pp. 32–40, 2012.

[17] L. Tian, Y. Fu, J. Xu, H. Li, and W. Ding, "The influence of speed on material removal mechanism in high speed grinding with single grit," *International Journal of Machine Tools and Manufacture*, vol. 89, pp. 192–201, 2015.

[18] C. Su, X. Mi, X. Sun, and M. Chu, "Simulation study on chip formation mechanism in grinding particle reinforced Cu-matrix composites," *International Journal of Advanced Manufacturing Technology*, vol. 99, no. 5–8, pp. 1249–1256, 2018.

[19] T. Tawakoli, H. Kitzig, and R. D. Lohner, "Experimental investigation of material removal mechanism in grinding of alumina by single grain scratch test," *Advanced Materials Research*, vol. 797, pp. 96–102, 2013.

[20] V. Singh, S. Ghosh, and P. V. Rao, "Comparative study of specific plowing energy for mild steel and composite ceramics using single grit scratch tests," *Materials and Manufacturing Processes*, vol. 26, no. 2, pp. 272–281, 2011.

[21] V. Singh, U. S. P. Durgumahanti, P. V. Rao, and S. Ghosh, "Specific ploughing energy model using single grit scratch test," *International Journal of Abrasive Technology*, vol. 4, no. 2, pp. 156–173, 2011.

[22] X. Chen and T. T. Öpöz, "Characteristics of material removal processes in single and multiple cutting edge grit scratches," *International Journal of Abrasive Technology*, vol. 6, no. 3, pp. 226–242, 2014.

[23] B. Denkena, J. Kohler, and F. Seiffert, "Machining of reinforced concrete using grinding wheels with defined grain pattern," *International Journal of Abrasive Technology*, vol. 4, no. 2, pp. 101–116, 2011.